

# Coordination Framework for Integrated Operation of Water-Power Systems under Contingencies

Mohannad Alhazmi, *Student Member, IEEE*, Payman Dehghanian, *Senior Member, IEEE*, Mostafa Nazemi, *Student Member, IEEE*, Fei Wang, *Senior Member, IEEE* and Abdullah Alfadda

**Abstract**—With the sharply-growing complexity and rapid deployment of smart technologies in our modern society, there is an urgent call for risk-aware management and coordination in day-to-day operation of the interlinked critical infrastructures. In particular, the interconnected Water and Power Systems (WaPS) stands out, urgently in need of joint and cooperative operation to maximize the economic benefits during normal operating conditions and resilience services during emergencies. The interdependency of WaPS is crucial for emergency response to High Impact Low Probability (HILP) incidents, the frequency and intensity of which have been recently on the rise. While contingency analysis is used to assist the system operators in gaining knowledge of the system's static security, such understanding is more challenging to achieve in the case of integrated WaPS. This paper proposes a novel optimization model for under-emergency operation of the integrated WaPS, considering contingencies in both networks. In order to ensure the delivery of water demand, the proposed formulation considers the hydraulic constraints of the water networks, which is naturally a nonlinear model. The proposed nonlinear model is approximated using a piece-wise linearization approach to convert the optimization model into a mixed-integer linear programming (MILP) formulation. The proposed analysis is applied to a modified IEEE 24-bus reliability test system that is jointly operated with two commercial-scale water networks. The proposed model is evaluated using various disaster severity levels, revealing significant resilience benefits.

**Index Terms**—Water-energy nexus (WEN); water and power systems (WaPS); emergency response; contingency analysis; interdependent networks; optimal power flow (OPF).

## NOMENCLATURE

### A. Sets

$g \in NG$	Set of system generating units.
$t \in NT$	Set of time intervals.
$n \in B$	Set of system buses.
$k \in L$	Set of system transmission lines.
$r \in \mathbf{R}$	Set of water system reservoirs.
$p \in \mathcal{P}$	Set of water system pumps.
$s \in \mathbf{S}$	Set of water system pipes.

### B. Variables and Functions

$P_t^{sh}$	The shedding amount of load at time $t$ .
------------	---

M. Alhazmi, P. Dehghanian and M. Nazemi are with the Department of Electrical and Computer Engineering, George Washington University, Washington, DC 20052, USA (e-mail: alhazmi@gwu.edu; payman@gwu.edu; mostafa\_nazemi@gwu.edu).

F. Wang is with the Electrical Engineering Department at the North China Electric Power University, Baoding 071003, China (email: fei-wang@ncepu.edu.cn).

A. Alfadda is with the Center of Excellence for Telecommunication Applications, King Abdulaziz City for Science and Technology, Riyadh 12354, Saudi Arabia (e-mail:aalfadda@kacst.edu.sa)

$Q_t$	Water flow rate at time $t$ .
$R_t^r$	Vector of reservoirs' water inflow rate for each reservoir $r$ at time $t$ .
$Q_t^j$	Water flow rate through pipe $j$ at time $t$ .
$Q_t^p$	Water flow rate through pump $p$ at time $t$ .
$H_t$	Pressure heads at time $t$ .
$H_{n,t}^j$	Pressure heads associated with pipe $j$ and node $n$ at time $t$ .
$H_{n,t}^p$	Pressure heads associated with pump $p$ and node $n$ at time $t$ .
$H_t^r$	Pressure heads associated with reservoir $r$ at time $t$ .
$Sign(\cdot)$	Sign function.
$\Delta E_t$	The difference of tanks' inflow/outflow rate at time $t$ .
$T_t^{in}$	Vector of water inflow to tanks at time $t$ .
$T_t^{out}$	Vector of water outflow to tanks at time $t$ .
$V_t$	Volume of stored water in tanks at time $t$ .
$W_t$	Pumps' speed at time $t$ .
$P_t^p$	Power consumption for pump $p$ at time $t$ .
$P_{b,t}^{p,adj}$	Vector of water electricity consumption in bus $b$ at time $t$ .
$X_t^{i,j}$	Continuous decision variable for pressure head breakpoint $i$ associated with pipe $j$ at time $t$ .
$X_t^{u,m,p}$	Continuous decision variable for pressure head breakpoint $u$ associated with pump $p$ at time $t$ .
$P_{g,t}$	Expected power output of generating unit $g$ at time $t$ .
$P_{knm,t}$	Power flow through transmission line $k$ (connecting bus $n$ to $m$ ) at time $t$ .
$P_{dn,t}$	Total power-water demand at time $t$ (MW).
$\theta_{i,t}$	Voltage angle for bus $i$ at time $t$ .

### C. Binary Variables

$Y_t^{i,j}$	Binary variable for pressure head breakpoint $i$ associated with pipe $j$ at time $t$ .
$H_{i,m,p,t}^{Upper}$	Binary variable for the upper triangle in the rectangle at time $t$ .
$H_{i,m,p,t}^{Lower}$	Binary variable for the lower triangle in the rectangle at time $t$ .
$\phi_{g,t}$	Binary variable for the connection status of generator $g$ at time $t$ (1 if it is available, 0 otherwise).

$\nu_{k,t}$	Binary variable for the connection status of power line $k$ at time $t$ (1 if it is online, 0 otherwise).
$\tau_t^p$	Binary variable for the connection status of pump stations $p$ at time $t$ (1 if it is online, 0 otherwise).

#### D. Parameters

$P_{d,t}$	Total electricity demand at time $t$ .
$\overline{P_{dn}}, \underline{P_{dn}}$	Maximum/Minimum electricity demand.
$x_k$	Reactance of transmission line $k$ .
$P_k^{max}$	Maximum power flow limit of line $k$ .
$P_g^{max}$	Maximum capacity limit of generating unit $g$ .
$P_g^{min}$	Minimum capacity limit of generating unit $g$ .
$D_t$	Vector of water demand ( $m^3/s$ ) at time $t$ .
$\hat{H}$	Reservoirs' geographical height.
$V_{min}$	Tanks' minimum volume.
$V_{max}$	Tanks' Maximum volume.
$\underline{\Delta E}$	Minimum charging/discharging difference for tanks.
$\overline{\Delta E}$	Maximum charging/discharging difference for tanks.
$r_p$	Pipe parameter.
$H_{min}$	Minimum nodal pressure heads.
$H_{max}$	Maximum nodal pressure heads.
$Q_{max/min}$	Maximum/Minimum water flow rate to the network.
$P_{max/min}^p$	Maximum/Minimum power consumption for pump $p$ .
$q_i^p$	Water flow rate of breakpoint $i$ for pump $p$ .
$q_i^j$	Water flow rate of breakpoint $i$ for pipe $j$ .
$c_t^{sh}$	The price of shedding load at time $t$ .
$c_{r,t}$	Vector of reservoirs' water price at time $t$ .
$c_{g,t}$	linear cost coefficients of generating unit $g$ at time $t$ (\$/MW).
$w_i^p$	Speed breakpoint $i$ for pump $p$ .
$a_{1,2,3}, z_{1,2}$	Performance parameters for pumps.
$C$	Incidence matrix of pumps' location.

## I. INTRODUCTION

**P**OWER and water networks are known among the most critical interconnected infrastructures due to their crucial role in human life and our modern society. Water networks are considered the most energy-intensive shareholder of the total electricity demand [1]. Approximately 4% of the electricity consumption in the United States is utilized by water networks around the country [2]. Drinking water and wastewater account for around 40% of the consumed energy for local governments [3]. Furthermore, water networks in California absorb around 20% of the total electricity consumed [4]. Therefore, there is an urgent need to improve the water networks' operation reliability and resiliency, i.e., water treatment, water purification, cooling, wastewater, etc., as the demanded electricity associated with water facilities is projected to increase due to the sharp rise in the population and use in industry applications.

In the traditional practice, water and power systems (WaPS) have been designed and planned as two separate and uncoupled systems, while in reality, the operation of both systems is jointly interdependent [5]. Power system operators are in need of water for refining fuels and generating electricity, while on the other hand, water facilities require electricity in order to operate normally. Further, the operation of mutually interdependent power and water systems is more critical and challenging in the case of limited availability of resources or failures in either network. If a shortage in delivering the demanded electricity is realized, water networks may not be supplied with sufficient energy required for pumping the water through pipelines, resulting in a failure in both networks. This interrelationship ecosystem of water and power is commonly known as water-energy nexus (WEN) [6]–[8].

Predominantly, the WEN has been investigated in the literature regarding policy, regulatory challenges, and its connections to economic growth and climate change [9]–[11]. Reference [12] studied the impact of climate change on water reservoir management and hydropower plant operation. A literature review on water distribution network optimization with respect to WEN is studied in [13]. A physics-based approach for modeling WEN to optimize the structure of water, wastewater, and power systems is studied in [14]. WEN linkage analysis is investigated in [15] to illustrate the effect of considering the interaction of coupled WaPS on various economic sectors. Optimal dispatch of WaPS and its impact on battery storage is studied in [16]. WaPS economic dispatch is employed in [17], focusing on the network's supply side. Reference [18] studied the economic dispatch of WaPS considering the energy management of various building applications. The demand response and frequency regulation of the water network are investigated in [19]. Reference [20] studied the operational resilience of WaPS under the condition of limited availability of water and/or energy. Focusing on the operation of WEN from the power system point of view, the utilization of energy flexibility through coordination of WaPS is investigated in [21]. Reference [22] studied the integration of WaPS using DC optimal power flow. Modeling such interconnected infrastructures individually is not preferred as it may result in sub-optimal solutions in both networks. Joint operation of WaPS using a different mechanism of power flow is investigated in [23]. The aforementioned studies investigated the operation of WaPS in different sectors under normal operating conditions in both networks, yet failed to study the operation of WaPS under emergency scenarios (i.e., outages in power system transmission lines and/or outages in water network pipelines).

The operation of WaPS faces growing challenges and vulnerability in the face of uncertain high impact low probability (HILP) events that cause damages to both networks, resulting in a partial or entire blackout in the systems. Lack of coordination between power and water systems under emergency operating conditions may cause a delay in the recovery of both systems. Such lack of coordination was experienced during the hurricane Maria in Puerto Rico [24]. The hurricane Maria caused damage to nearly 90% of the power network in Puerto Rico, and various locations were not supplied with demanded water for a long time due to the severance of the hurricane

and the absence of coordination between several interlinked sectors, e.g., power and water operators, which caused a delay in the response and recovery of both systems [25], [26].

Different from the state-of-the-art models, where the operation of WaPS is modeled and studied assuming normal operating conditions of the systems, this paper bridges the gap in co-optimization and joint operation of water and power systems under emergency operating conditions. We propose a computationally-efficient mixed-integer linear programming (MILP) formulation that jointly optimizes the operation of both networks in presence of different contingencies in both power and water networks and under various disaster severity levels. The proposed formulation captures the contingencies in power system generators, transmission lines, and water networks. The presented model aims to enhance flexibility and advance the resilience of the joint WaPS in the face of infrastructure failures and extreme HILP events.

The rest of the paper is organized as follows. Section II presents the proposed contingency-responsive joint optimization framework of power-water systems considering the complete hydraulic constraints of the water network. Numerical case studies and simulation results on a modified IEEE 24-bus reliability test system jointly operated with two 15-node water networks are presented in Section III. The paper is concluded in Section IV.

## II. PROPOSED METHODOLOGY

This section presents the proposed mathematical model for contingency analysis in a jointly-operated WaPS. The proposed model of the water network consists of reservoirs, pipes, pumps, and tanks, which is mathematically represented using a directed graph  $G = (\mathcal{N}, \mathcal{A})$ , where  $\mathcal{N}$  denote the set of  $N$  water network nodes representing  $R$  reservoirs and  $T$  tanks.  $\mathcal{A}$  is the set of  $A$  arcs, which consists of pipes and pumps. Water flow rate  $q$  is maintained by increasing the pressure head, using pump stations, or by adequate elevation difference between two nodes, such that if the water network is supplied by groundwater and the gravity is insufficient, a pumping station is needed to increase the pressure head and facilitate the flow of water. The water flow direction is determined by the water flow rate's positive and negative values  $q$ . Water networks' schematic diagram and their hydraulic components are demonstrated in Fig. 1.

### A. Objective Function

The WaPS operation objective during emergency operating conditions is to minimize the total cost of the system in the presence of contingencies. Therefore, the objective function is modeled by minimizing the cost of load outages and power generation in WaPS, formulated as follows:

$$\min \sum_{t=1}^{NT} \sum_{g=1}^{NG} \sum_{i=1}^{\mathcal{D}} \sum_{r=1}^{\mathcal{R}} \left( c_{i,t}^{sh} P_{i,t}^{sh} + c_{g,t} P_{g,t} + c_{r,t} R_t^r \right) \quad (1)$$

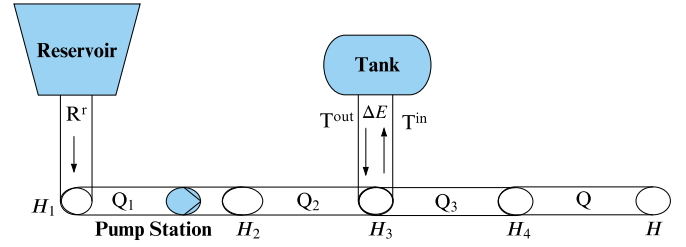


Fig. 1. Schematic diagram of the water network components.

### B. WaPS Integration and Contingency Constraints

The contingencies in power systems are modeled within the DC optimal power flow (DCOPF) mechanism and is jointly formulated with the water network as follows:

$$P_{b,t}^{p,adj} = \sum_{p=1}^P C P_t^p \quad \forall b, \forall t \quad (2)$$

$$P_{dn,t} = P_{d,t} + P_{b,t}^{p,adj} \quad \forall n, \forall t \quad (3)$$

$$\underline{P}_{dn} \leq P_{d,t} + P_{b,t}^{p,adj} \leq \overline{P}_{dn} \quad \forall n, \forall t \quad (4)$$

$$P_{k,t} = \frac{\theta_{n,t} - \theta_{m,t}}{x_k} \quad \forall k, \forall t \quad (5)$$

$$-P_k^{max} \nu_{k,t} \leq P_{knm,t} \leq P_k^{max} \nu_{k,t} \quad \forall k, \forall t \quad (6)$$

$$p_g^{min} \phi_{g,t} \leq P_{g,t} \leq P_g^{max} \phi_{g,t} \quad \forall t \quad (7)$$

$$\sum_{g \in NG} P_{g,t} + \sum_{i \in \mathcal{D}} P_{i,t}^{sh} - \sum_{k \in L} P_{k,t} = \sum_{d \in \mathcal{D}} P_{dn,t} \quad \forall t \quad (8)$$

$$0 \leq P_{i,t}^{sh} \leq P_{dn,t} \quad \forall i \in \mathcal{D}, n, \forall t. \quad (9)$$

$$P_{min}^p \tau_t^p \leq P_t^p \leq P_{max}^p \tau_t^p \quad \forall p, \forall t \quad (10)$$

Constraint (2) adjusts the dimension of pump electricity consumption, while constraint (3) integrates the water network's electricity consumption with power system demand. Total demand for the joint WaPS is bounded in (4). The power flow in transmission lines is introduced in (5) and bounded to its maximum and minimum limits in (6), considering the availability status of lines  $\nu_{k,t}$ . Constraint (7) limits the output of each power generating unit to its maximum and minimum capacities, where  $\phi_{g,t}$  identifies the status of generation units. Power balance constraint considering the load outage in WaPS is described in (8). The interrupted load is bounded above in (9) not to exceed the nodal load demand in normal operating conditions. The availability status of water pump stations is bounded in (10).

### C. Water Flow Constraints

Water demand is delivered to customers through a network of pipes, pumps, and tanks. During peak hours, tanks are utilized to smoothen the pumpage demand to assist the water network during emergency scenarios. The water flow hydraulic constraints are modeled as follows:

$$R_t^r - D_t - Q_t - \Delta E_t = 0 \quad \forall t \quad (11)$$

$$-Q_{max} \leq Q_t \leq Q_{max} \quad \forall t \quad (12)$$

$$Q_t^p \geq 0 \quad \forall t \quad (13)$$

$$H_{n,t} - H_{n+1,t} = r_p |Q_t^j|^{1.852} \text{Sign}(Q_t^j) \quad \forall t \quad (14)$$

$$H_t^r - \hat{H} = 0 \quad \forall t \quad (15)$$

$$H_{min} \leq H_t \leq H_{max} \quad \forall t \quad (16)$$

$$V_{t+1} = V_t + \Delta E_t \quad \forall t \quad (17)$$

$$\Delta E_t = T_t^{in} - T_t^{out} \quad \forall t \quad (18)$$

$$\underline{\Delta E} \leq \Delta E_t \leq \overline{\Delta E} \quad \forall t \quad (19)$$

$$V_t = S_a h_t \quad \forall t \quad (20)$$

$$V_{min} \leq V_t \leq V_{max} \quad \forall t \quad (21)$$

$$\Delta H_t = W_t \left( a_1 - a_2 \left( \frac{Q_t}{W_t} \right)^{a_3} \right) \quad \forall t \quad (22)$$

$$P_t^p = W_t^3 \left( z_1 - z_2 \left( \frac{Q_t}{W_t} \right) \right) \quad \forall t \quad (23)$$

The dynamic flow balance in the water network is formulated in (11). Water flow through pipelines and pumps are bounded in (12) and (13), respectively. The Hazen–Williams formula [27] is used in (14) to model the flow of water through pipes. Constraints (15) set the pressure head at the reservoir node to its geographical heights. Nodal pressure head is limited in (16). The dynamic operation of water flow in tanks is modeled in (17). Constraints (18) defines  $\Delta E_t$ , which governs the difference between charging and discharging water flow of tanks.  $\Delta E_t$  is limited in (19). Constraints (20) formulates the pressure head at the tank nodes, which is driven by the water stored in the related tanks. The volume of each tank is bounded in (21). Water pumps increase the nodal head pressure to increase the water flow. The controlled increase of pressure by pumps is formulated in (22). Pumps electricity consumption is modeled in (23) and bounded in (10) to its maximum and minimum electricity consumption.

Non-linearity is presented in constraints (14), (23) and (10). Solving nonlinear programming (NLP) might be time-intensive, and an optimal feasible solution might not be guaranteed in large-scale water networks. A piece-wise linear formulation [28] is applied to convert the NLP model to tractable

mixed-integer linear programming (MILP) constraints. The approximated linearized constraints are modeled as follows:

$$\sum_{i=1}^{I-1} Y_t^{i,j} = 1 \quad \forall j, \forall t \quad (24)$$

$$X_t^{i,j} \leq Y_t^{i-1,j} + Y_t^{i,j} \quad \forall j, \forall i, \forall t \quad (25)$$

$$\sum_{i=1}^I X_t^{i,j} = 1 \quad \forall j, \forall t \quad (26)$$

$$X_t^{I,j} \leq Y_t^{I-1,j} \quad \forall j, \forall t \quad (27)$$

$$X_t^{1,j} \leq Y_t^{1,j} \quad \forall j, \forall t \quad (28)$$

$$Q_t^j = \sum_{i=1}^I X_t^{i,j} q_i^j \quad \forall j, \forall t \quad (29)$$

$$H_{n,t}^j - H_{n+1,t}^j = \sum_{i=1}^I X_t^{i,j} \Delta H_t^j(q_i^j) \quad \forall j, \forall t \quad (30)$$

$$\sum_{u=1}^U \sum_{m=1}^M X_t^{u,m,p} = 1 \quad \forall p, \forall t \quad (31)$$

$$Q_t^p = \sum_{u=1}^U \sum_{m=1}^M X_t^{u,m,p} q_u^p \quad \forall p, \forall t \quad (32)$$

$$W_t = \sum_{u=1}^U \sum_{m=1}^M X_t^{u,m,p} w_m^p \quad \forall p, \forall t \quad (33)$$

$$\Delta H_t^p = \sum_{u=1}^U \sum_{m=1}^M \Delta H_t^p(q_u^p, w_m^p) X_t^{u,m,p} \quad \forall p, \forall t \quad (34)$$

$$P_t^p = \sum_{u=1}^U \sum_{m=1}^M P_t^p(q_u^p, w_m^p) X_t^{u,m,p} \quad \forall p, \forall t \quad (35)$$

$$\sum_{u=1}^U \sum_{m=1}^M (H_{u,m,p,t}^{Upper} + H_{u,m,p,t}^{Lower}) = 1 \quad \forall p, \forall t \quad (36)$$

$$\begin{aligned} X_t^{u,m,p} \leq & H_{u,m-1,p,t}^{Upper} + H_{u+1,m,p,t}^{Upper} + H_{u,m,p,t}^{Upper} \\ & + H_{u-1,m,p,t}^{Lower} + H_{u,m+1,p,t}^{Lower} + H_{u,m,p,t}^{Lower} \quad \forall u, \forall m, \forall p, \forall t \end{aligned} \quad (37)$$

Constraints (24)-(30) represent the linear approximation for the nonlinear constraint (14). Constraints (24) drives only one binary variable to take the value of 1, while (25)-(28) indicate that only non-zero values are selected for  $X_t^{i,j}$  and  $X_t^{i+1,j}$ . Pressure head difference for pipes is ensured to be selected appropriately to evaluate the approximated functions in constraints (29)-(30). The linearized formulation of the nonlinear constraints (22)-(23) is modeled using the triangle

technique in (31)–(37). Constraint (31) presents the weight of the convex combination of the selected triangle. The linear combinations of any selected values for water flow through pumps and pump’s speed are modeled in (32) and (33), respectively, while the bi-variate nonlinear functions for each pump’s pressure difference and electricity consumption are approximated in (34) and (35) respectively. Only one triangle is forced to be selected in constraint (36) for the convex combination, and constraint (37) ensures that only values other than zero of  $X_t^{i,m,p}$  can be associated with all three vertices of the triangle. Detailed illustration of the linearization technique is provided in [23].

The complete formulation for the integrated WaPS in the form of a MILP optimization model is presented in the following, which considers the contingency-driven emergency response in the joint operation of WaPS.

$$\begin{aligned} & \min (1) \\ & \text{subject to } (2) - (13), (15) - (21), (10) - (37) \end{aligned}$$

### III. NUMERICAL CASE STUDIES

#### A. System Descriptions, Data, and Assumptions

The proposed formulation for the resilient operation of the interconnected power and water networks under contingency scenarios is applied on a modified IEEE 24-bus reliability test system jointly operated and connected to two commercial-scale water networks. The IEEE 24-bus reliability test system consists of 12 generating units, 34 transmission lines, and 17 load points. Each water network consists of 15 nodes connected to a power grid load point, as shown in Fig. 3. Each water network consists of 15 nodes, i.e., 11 pipelines, 3 pumps, and 2 tanks, and is connected to a power grid load point. The precise locations for each water network component, e.g., pumping stations, water tanks, water demand nodes, etc., are illustrated in Fig. 2. The initial volume of all water tanks is set to zero. All data for the studied WaPS (i.e., generation capacity, load profiles, transmission line parameters, water demand profiles, pipeline parameters, etc.) are provided in [29], [30]. The simulations are performed using CPLEX solver to handle the reformulated MILP model. A Mathematical Programming Language (AMPL) environment [31], using a PC with an Intel Xeon E5-2620 v2 processor, 16 GB of memory, and 64-bit operating system, is used to perform all the simulations.

#### B. Results and Discussions

In order to demonstrate the performance of the proposed model, three different case studies are presented:

- **Case Study I (CS-I)** presents the *day-ahead normal operation* of the proposed WaPS, which integrates water networks’ and the power network’s operations jointly and interdependently, where the DCOPF mechanism and hydraulic water constraints are efficiently merged.
- **Case Study II (CS-II)** models the N-1 contingency analysis for the joint operation of the WaPS, taking into account the DCOPF mechanism for the power network and water network hydraulic model in emergency states.

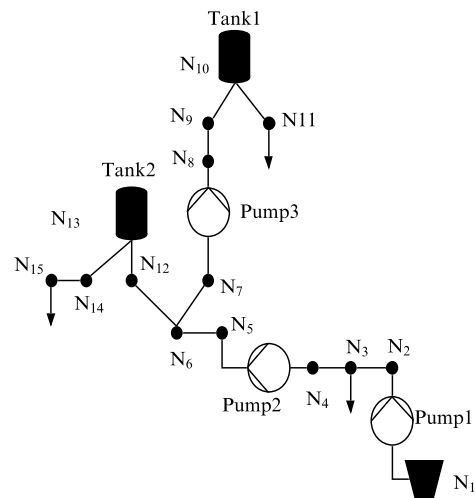


Fig. 2. Schematic diagram of the commercial-scale 15-node water network.

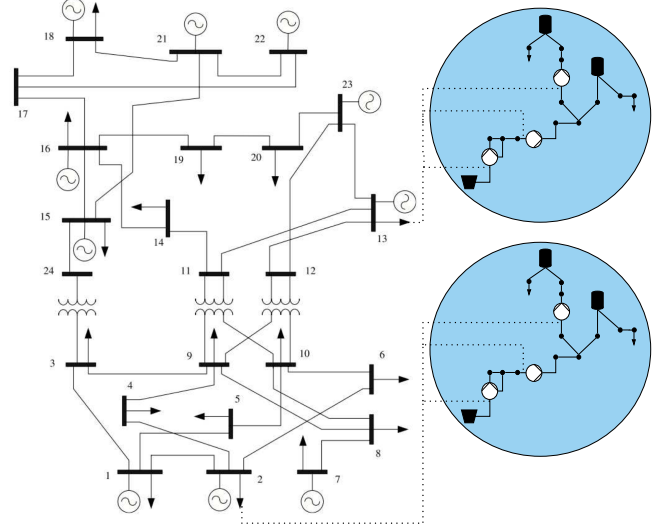


Fig. 3. Schematic diagram of the IEEE 24-bus reliability test system supplying two water networks.

TABLE I  
TOTAL OPERATION COST AND OPTIMIZATION COMPUTATION TIME IN DIFFERENT TEST CASES

Case #	Operation Cost (\$)	Time (sec.)
CS-I	42,348.17	92.1
CS-II	45,113.22	123.2
CS-III	47,234.72	149.2

- **Case Study III (CS-III)** represents the joint operation of the WaPS under a higher (e.g., level-2) disaster severity, i.e., N-2 contingency analysis, taking into account simultaneous failures in two power transmission lines, thereby emergency operation of WaPS.

Figure 4 illustrates the day-ahead electricity consumption of water pumps in CS-I, when the joint WaPS operates normally. Water tanks’ performance for the 24-hour operation period is shown in Fig. 5. It can be observed from Fig. 5 that water tanks are assisting the water network during peak hours (e.g.,

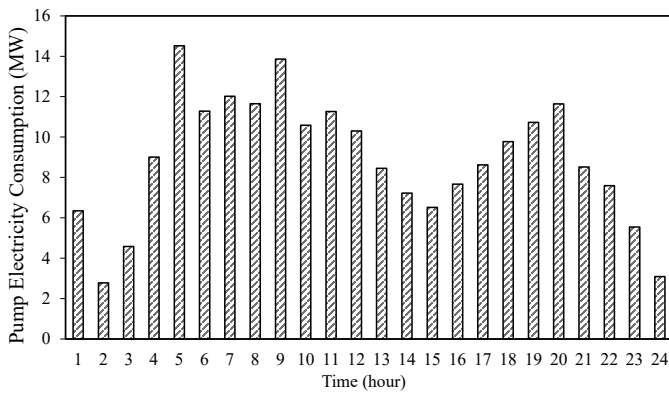


Fig. 4. Scheduled electricity consumption of water pumps in normal operating conditions: CS-I.

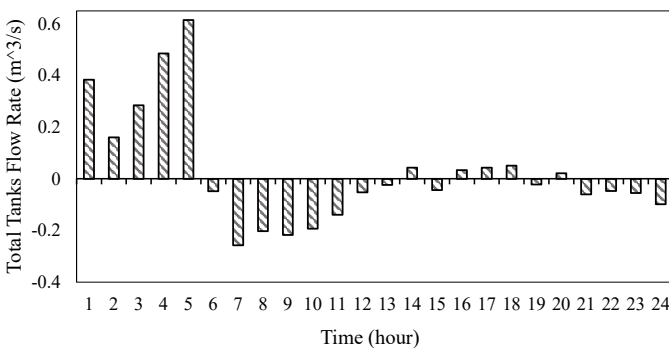


Fig. 5. Scheduled tanks water flow rate in normal operating conditions: CS-I.

hours 7-13) by discharging (negative value) and supplying the water demand, while it's charging (positive value) during off-peak hours (e.g., hours 1-7). The daily load profile for the integrated WaPS in **CS-I** is shown in Fig. 6. In the case of emergency response, i.e., **CS-II** and **CS-III**, the amount of load shed at each hour is demonstrated in Fig. 7.

The operational cost for all case studies and the computational results are presented in Table I. The total operating cost for **CS-I**, when normal operation of the joint WaPS is studied, is reported at \$42,348.17. The optimal operation cost for the interlinked WaPS, taking into account the failure of one line (i.e., N-1 scenarios) in **CS-II** and N-2 scenarios in **CS-III**, are reported at \$45,113.22 and \$47,234.72, respectively. The computation time for **CS-I** is reported 92.1 seconds, while that of the **CS-II** and **CS-III** are recorded at 123.2 seconds and 149.2 seconds, respectively. It can be observed that the proposed solution is computationally-efficient to be used for the integrated operation of WaPS under emergencies.

#### IV. CONCLUSION

Different from the state-of-the-art models, this paper proposed a novel framework for the joint and coordinated operation of the water and electricity networks under contingency scenarios. In order to comprehensively evaluate the effectiveness of the interconnected WaPS, the DCOPF mechanism and hydraulic water system operation have been taken into account.

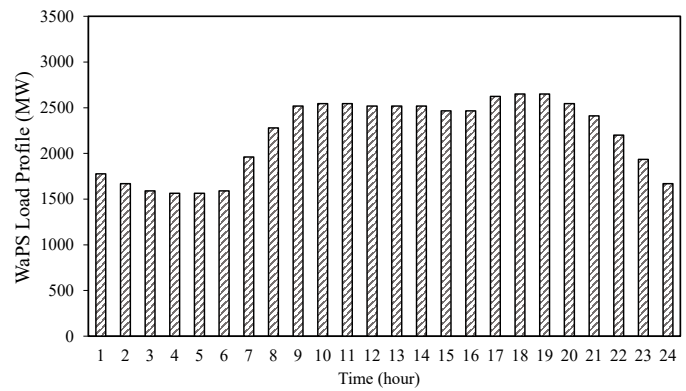


Fig. 6. Load Profile for the integrated WaPS in normal operating conditions: CS-I.

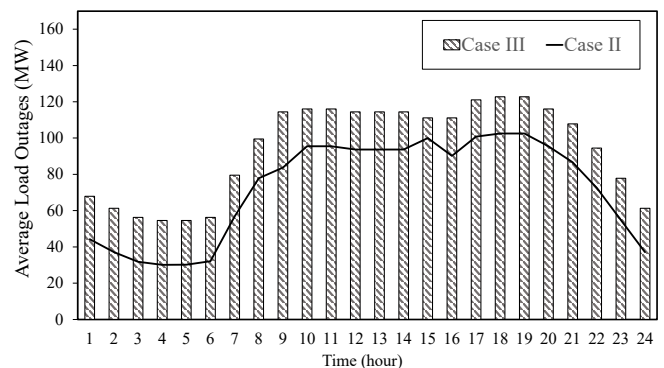


Fig. 7. Average load outage in WaPS when contingencies are applied.

Piece-wise linearization technique was used to approximate the hydraulic water constraints and convert the NLP model to a tractable mixed-integer linear programming (MILP) formulation, which commercial off-the-shelf solvers can quickly solve. The proposed model was applied to and studied on two commercial-scale water networks, each consisting of 15 nodes, which are jointly supplied and operated with the IEEE 24-bus reliability power test system. The simulation results included both N-1 and N-2 contingency scenarios and verified the promising performance of the proposed integrated WaPS model in enhancing the performance reliability and resilience of the critical WaPS infrastructures when facing failures and threatening HILP emergencies.

#### REFERENCES

- [1] V. M. Leiby and M. E. Burke, *Energy efficiency best practices for North American drinking water utilities*. WRF, 2011.
- [2] B. Appelbaum, R. Goldstein, and W. Smith, "Water & sustainability: Us electricity consumption for water supply & treatment—the next half century," *Electric Power Research Institute, EPRI, Palo Alto, CA, USA*, 2002.
- [3] C. Copeland and N. T. Carter, "Energy-water nexus: The water sector's energy use," 2014.
- [4] G. Klein, M. Krebs, V. Hall, T. O'Brien, and B. Blevins, "California's water-energy relationship," *California Energy Commission*, pp. 1–180, 2005.

- [5] S. Shin, S. Lee, D. R. Judi, M. Parvania, E. Goharian, T. McPherson, and S. J. Burian, "A systematic review of quantitative resilience measures for water infrastructure systems," *Water*, vol. 10, no. 2, p. 164, 2018.
- [6] X. Zhang and V. V. Vesselinov, "Energy-water nexus: Balancing the tradeoffs between two-level decision makers," *Applied energy*, vol. 183, pp. 77–87, 2016.
- [7] Q. Li, S. Yu, A. Al-Sumaiti, and K. Turitsyn, "Modeling a micro-nexus of water and energy for smart villages/cities/buildings," *arXiv preprint arXiv:1711.03241*, 2017.
- [8] A. Santhosh, A. M. Farid, and K. Youcef-Toumi, "Optimal network flow for the supply side of the energy-water nexus," in *2013 IEEE International Workshop on Intelligent Energy Systems (IWIES)*. IEEE, 2013, pp. 155–160.
- [9] C. A. Scott, S. A. Pierce, M. J. Pasqualetti, A. L. Jones, B. E. Montz, and J. H. Hoover, "Policy and institutional dimensions of the water-energy nexus," *Energy Policy*, vol. 39, no. 10, pp. 6622–6630, 2011.
- [10] C. Ringler, A. Bhaduri, and R. Lawford, "The nexus across water, energy, land and food (welf): potential for improved resource use efficiency?" *Current Opinion in Environmental Sustainability*, vol. 5, no. 6, pp. 617–624, 2013.
- [11] U. Lele, M. Klousia-Marquis, and S. Goswami, "Good governance for food, water and energy security," *Aquatic procedia*, vol. 1, pp. 44–63, 2013.
- [12] S.-C. Kao, M. J. Sale, M. Ashfaq, R. U. Martinez, D. P. Kaiser, Y. Wei, and N. S. Diffenbaugh, "Projecting changes in annual hydropower generation using regional runoff data: An assessment of the united states federal hydropower plants," *Energy*, vol. 80, pp. 239–250, 2015.
- [13] N. Vaklifard, M. Anda, P. A. Bahri, and G. Ho, "The role of water-energy nexus in optimising water supply systems—review of techniques and approaches," *Renewable and Sustainable Energy Reviews*, vol. 82, pp. 1424–1432, 2018.
- [14] W. N. Lubega and A. M. Farid, "Quantitative engineering systems modeling and analysis of the energy–water nexus," *Applied Energy*, vol. 135, pp. 142–157, 2014.
- [15] D. Fang and B. Chen, "Linkage analysis for the water–energy nexus of city," *Applied energy*, vol. 189, pp. 770–779, 2017.
- [16] A. Santhosh, A. M. Farid, and K. Youcef-Toumi, "The impact of storage facility capacity and ramping capabilities on the supply side economic dispatch of the energy–water nexus," *Energy*, vol. 66, pp. 363–377, 2014.
- [17] —, "Real-time economic dispatch for the supply side of the energy-water nexus," *Applied Energy*, vol. 122, pp. 42–52, 2014.
- [18] F. Moazeni, J. Khazaei, and A. Asrari, "Step towards energy-water smart microgrids; buildings thermal energy and water demand management embedded in economic dispatch," *IEEE Transactions on Smart Grid*, pp. 1–1, 2021.
- [19] K. Oikonomou, M. Parvania, and R. Khatami, "Optimal demand response scheduling for water distribution systems," *IEEE Transactions on Industrial Informatics*, vol. 14, no. 11, pp. 5112–5122, 2018.
- [20] S. Zuloaga, P. Khatavkar, L. Mays, and V. Vittal, "Resilience of cyber-enabled electrical energy and water distribution systems considering infrastructural robustness under conditions of limited water and/or energy availability," *IEEE Transactions on Engineering Management*, pp. 1–17, 2019.
- [21] K. Oikonomou and M. Parvania, "Optimal coordination of water distribution energy flexibility with power systems operation," *IEEE Transactions on Smart Grid*, vol. 10, no. 1, pp. 1101–1110, 2018.
- [22] M. Alhazmi, P. Dehghanian, M. Nazemi, and M. Mitolo, "Joint operation optimization of the interdependent water and electricity networks," in *2020 IEEE Industry Applications Society Annual Meeting*. IEEE, 2020, pp. 1–7.
- [23] M. Alhazmi and P. Dehghanian, "Optimal integration of interconnected water and electricity networks," *IET Generation, Transmission & Distribution*, 2021.
- [24] P. Brown, C. M. V. Vega, C. B. Murphy, M. Welton, H. Torres, Z. Rosario, A. Alshawabkeh, J. F. Cordero, I. Y. Padilla, and J. D. Meeker, "Hurricanes and the environmental justice island: Irma and maria in puerto rico," *Environmental Justice*, vol. 11, no. 4, pp. 148–153, 2018.
- [25] R. Subramanian, A. Ellis, E. Torres-Delgado, R. Tanzer, C. Malings, F. Rivera, M. Morales, D. Baumgardner, A. Presto, and O. L. Mayol-Bracero, "Air quality in puerto rico in the aftermath of hurricane maria: a case study on the use of lower cost air quality monitors," *ACS Earth and Space Chemistry*, vol. 2, no. 11, pp. 1179–1186, 2018.
- [26] Y. Lin, M. Sevillano-Rivera, T. Jiang, G. Li, I. Cotto, S. Vosloo, C. M. Carpenter, P. Larese-Casanova, R. W. Giese, D. E. Helbling *et al.*, "Impact of hurricane maria on drinking water quality in puerto rico," *Environmental Science & Technology*, vol. 54, no. 15, pp. 9495–9509, 2020.
- [27] L. W. Mays, *Water resources engineering*. John Wiley & Sons, 2010.
- [28] C. D'Ambrosio, A. Lodi, and S. Martello, "Piecewise linear approximation of functions of two variables in mip models," *Operations Research Letters*, vol. 38, no. 1, pp. 39–46, 2010.
- [29] "Water network data information," <http://tiny.cc/GWU-SmartGridLab>, accessed: 2021-03-30.
- [30] "IEEE 24-bus RTS data information," <https://tinyurl.com/ypukrbfh>, accessed: 2021-03-30.
- [31] R. Fourer, D. M. Gay, and B. W. Kernighan, "Ampl. a modeling language for mathematical programming," 1993.